Available online at www.sciencedirect.com
SCIENCE DIRECT®
Journal of Power Sources 138 (2004) 340–350
JOURNAL OF POWER SOURCES
www.elsevier.com/locate/jpowsour

γ-Butyrolactone-acetonitrile solution of triethylmethylammonium tetrafluoroborate as an electrolyte for double-layer capacitors

M.S. Ding[a,*], K. Xu[a], J.P. Zheng[b], T.R. Jow[a]

[a] *Army Research Laboratory, Adelphi, MD 20783, USA*
[b] *Florida A&M and Florida State University, Tallahassee, FL 32310, USA*

Received 25 May 2004; accepted 20 June 2004
Available online 23 August 2004

Abstract

Properties of a γ-butyrolactone-acetonitrile solution of triethylmethylammonium tetrafluoroborate were systematically measured for its potential to be used as an electrolyte in double-layer capacitors and for demonstrating the ways in which these properties can be optimized through choosing an appropriate solvent mixture and an appropriate salt and adjusting the electrolyte composition. These properties included the liquid range of the solvent and the solution at different compositions, the dielectric constant of the binary solvent as a function of solvent composition and temperature, the conductivity of the solution as a function of salt content, solvent composition, and temperature and the oxidative stability of the electrolytes at different solvent compositions. To correlate the properties of the electrolytes with the properties and performance of the double-layer capacitors utilizing the electrolytes, such capacitors were built and their equivalent series resistance, cyclic voltammogram, and operating voltage were measured for different solvent compositions of the capacitor electrolytes. The results revealed a clear correlation between the conductivity and the oxidative stability of the electrolytes and the equivalent series resistance and the operating voltage of the capacitors, respectively. Furthermore, it is clearly demonstrated that by using a binary solvent and adjusting its composition properly, the electrolyte it makes with an appropriate salt can be effectively optimized with regard to its liquid range, conductivity, and electrochemical stability window, which in turn imparts the double-layer capacitor utilizing such an electrolyte with a set of optimal properties such as a wide range of operating temperature, low equivalent series resistance, and high operating voltage.

Keywords: Non-aqueous solvent; Electrolyte; Double-layer capacitor; Phase diagram; Electrolytic conductivity; Electrochemical stability

1. Introduction

An electrochemical double-layer capacitor is an energy storage device in which the storage is effected by accumulation of ions in the electrolyte near the electrode surfaces in response to an applied electrical field [1,2]. As this process involves only ions migrating through the electrolyte but not their interaction with the lattice of the electrode materials or undergoing chemical reactions as those in a battery must do, the speed at which a double-layer capacitor can operate is generally higher than a battery albeit with a lower storage density. For the same reason, a double-layer capacitor generally has considerably higher cycle life and efficiency than a battery. These properties make it advantageous for many applications to use a capacitor in parallel with a battery to produce a unit with improved speed, cycle life and efficiency than those of the two separate devices [3–5]. In particular, as an increase in the speed of migration of the ions in the electrolyte normally results in an increase in the speed of operation of the capacitor device, a high electrolytic conductivity has been a major goal for the formulation of electrolytes for the double-layer capacitors [1,2,4,6,7].

Closely related to the conductivity is the liquid range of the electrolyte, the relation being that a higher boiling point of a liquid generally signifies a higher viscosity and thereby, a lower conductivity if the liquid is an electrolyte [8]. For a solvent mixture or an electrolyte, the liquid range is limited

* Corresponding author. Tel.: +1 301 394 0272; fax: +1 301 394 0273.
E-mail address: mding@arl.army.mil (M.S. Ding).

0378-7753/$ – see front matter © 2004 Elsevier B.V. All rights reserved.
doi:10.1016/j.jpowsour.2004.06.039

on the upper end by its bubble point, above which the electrolyte becomes thermodynamically unstable with respect to a certain gaseous phase; this phase will evolve from the electrolyte if it is contained under a pressure of one atmosphere. Of course, a higher containing pressure could delay the vaporization of the electrolyte with regard to an increasing temperature. But that often will incur higher complexity in design and higher cost in production. On the other hand, an electrolyte with too high a bubble point, associated usually with a high viscosity, is expected to be poorly conductive. The bubble point of an electrolyte, therefore, is an important measure for both its abilities to operate at elevated temperature and to carry a heavy current [8].

The liquid range of an electrolyte is limited on the lower end by the liquidus temperature of the electrolyte, below which the electrolyte becomes, again, thermodynamically unstable, but this time with regard to a certain solid phase; this solid phase will precipitate in the presence of a suitable nucleating agent, of which carbon particles, unfortunately have been shown to be an effective member [9]. To make matters worse, the liquidus temperature is not easily predicted from the composition of the electrolyte and the melting points of the components. Therefore, liquidus temperatures of many important non-aqueous solvents for the batteries and capacitors have been mapped in the form of binary and multicomponent phase diagrams, mostly through measurements, but partly with thermodynamic modeling and computation [10–15].

Another critically important property of an electrolyte is its electrochemical stability window, which places a limit on the voltage within which the capacitor that employs the electrolyte can be operated without significant deterioration due to the electrochemical reactions. As the energy stored in a capacitor is proportional to the square of its operating voltage, electrolytes with wide electrochemical stability windows are highly desirable for use in the double-layer capacitors.

The main purpose of this report is to demonstrate how these important properties can be optimized for an electrolyte by forming it from an appropriate salt and an appropriate solvent mixture [16]. We do this with a model electrolyte system: the solution of triethylmethylammonium tetrafluoroborate (Et_3MeNBF_4:$(C_2H_5)_3CH_3NBF_4$) in the binary solvent of γ-butyrolactone (γBL:$C_4H_6O_2$) and acetonitrile (AN:C_2H_3N), by systematically measuring the change of dielectric constant of the solvent with its composition and temperature, of liquid range of the solvent and the electrolyte with their composition, of conductivity of the electrolyte with its composition and temperature, of electrochemical stability of the electrolyte with the solvent composition, and of the properties and performance of the capacitors with the solvent composition of the electrolyte used in the capacitors. The choice of using AN as one of the solvent components was due to its low viscosity and moderately high dielectric constant and solvating power, as listed in Table 1 [7,17–19], which have made it the most widely used non-aqueous solvent for double-layer capacitors [4,6,20,21]. But it has at the same time a low boiling point, a relatively low oxidative stability [20], and a freezing point that is not particularly low. γBL, the other solvent component and another commonly used solvent for capacitors [6,7,22], has a considerably better oxidative stability [20], a much higher boiling point, and a freezing point that is comparable to that of AN, as listed in Table 1. As for the salt Et_3MeNBF_4, it is a unique member of the quaternary ammonium salts that are the most widely used in making non-aqueous double-layer capacitors due to their desirable properties [6,21,23]. The Et_3MeNBF_4 derives its uniqueness from its wide electrochemical stability window and its high solubility in non-aqueous solvents due to the non-symmetrical configuration of the Et_3MeN^+ ion [23–25]. With these components and the electrolytes they make, we intend to show that by judiciously choosing a mixed solvent and a salt, it is possible, through proper formulation, to arrive at an electrolyte with a set of properties of which the majority are superior to those of the electrolytes formed by a salt and a single solvent. We also intend to show, with laboratory capacitors made from these electrolytes, how closely related the properties of the electrolytes are to the properties and performance of the capacitors that employ the electrolytes.

Table 1
Properties of acetonitrile (AN) and γ-butyrolactone (γBL) solvents

Solvent	θ_b (°C)	θ_m (°C)	$\varepsilon_{20\,°C}$	$\eta_{25\,°C}$ (mPa s)	DN (kcal mol^{-1})
AN	81.2	−43.4	36.64	0.369	14.1
γBL	204.8	−43.1	39.0	1.7164	15.9

Boiling point, θ_b; melting point, θ_m; dielectric constant, ε; viscosity, η; and donicity, DN. The temperature values are measured in this study, and the others are from literature.

2. Experimental

2.1. Sample preparation

The starting solvent AN of purity 99.9% was purchased from Aldrich, γBL of purity 99.9% from EM industries, and Et_3MeNBF_4 of purity 99.5% was prepared in our laboratory. The solvents were further dried with molecular sieves until the water content was 25 ppm for γBL and below 10 ppm for AN. In an argon-filled dry box, the γBL and AN were mixed to form eight mixtures $\gamma BL_{1-w}AN_w$ with solvent weight fraction w running from 0 to 1. In each of these solvents, Et_3MeNBF_4 was dissolved until the salt molality m exceeded 2.2 mol kg^{-1}. Conductivity measurement on these solutions and their subsequent dilution for the next set of less concentrated solutions were done in a dry room with a dew point of typically −70 °C.

2.2. Measurement of characteristic temperatures

A modulated differential scanning calorimeter (MDSC 2920, TA Instruments) cooled with liquid nitrogen was used to determine the melting and boiling points of the solvent

components and the solidus, liquidus, and bubble temperatures of the solvent mixtures. For the melting, solidus, and liquidus temperatures, a small amount of the mixture crimp-sealed in a pair of aluminum pan and lid (0219-0062, Perkin-Elmer Instruments) was first made to crystallize by cooling it below its eutectic point. It was then warmed up at a rate of 2 °C/min through its liquidus point, producing a heat flow curve from which the characteristic temperatures of the sample were determined on the endothermic peaks associated with the phase transitions. For the boiling and bubble points, the sample was crimped with an aluminum lid with a 50 μm hole in the middle (N519-0788, Perkin-Elmer) for allowing controlled escape of the sample vapor. The sample was heated through its bubble point (boiling point for a pure solvent) at 5 °C/min, and the boiling or bubble point was evaluated at the onset of the rapid heat absorption associated with the vaporization of the sample [8].

2.3. Measurement of dielectric constant and conductivity

Dielectric constant ε and electrolytic conductivity κ of the solvents were measured with an HP (now Agilent) 4284A precision LCR meter at selected temperatures within a Tenney Jr. Environmental Chamber, the whole measurement process being automated with a house-made program run on a personal computer and carried out in a dry room. Temperature θ (θ symbolizes temperature in °C and T in K [26]) of the measurements went from 60 to −50 °C in 10° decrements, stopping at each for an hour of thermal equilibration before a measurement. The measurement consisted of an impedance scan from 1 MHz to 20 Hz with an amplitude of 10 mV, from which an $\varepsilon'\varepsilon''$-plot or a $Z'Z''$-plot was made and ε or κ was evaluated from the impedance curve. The measurement cells were modified from a commercial conductivity cell (YSI 3402) consisting of a pair of dip-type platinum-iridium alloy electrodes of a nominal cell constant of 0.1 cm^{-1}, such that the liquid to be measured could be contained and sealed in the Pyrex cell body. The precision of such measurements, after proper calibration and correction, was estimated to be 0.5% for κ and 1% for ε [8,27].

2.4. Measurement of electrochemical stability

Electrochemical stability of the electrolytes, mostly against oxidation, was determined on the electrolytes of 1 m salt concentration using an EG&G 273A Potentiostat on a three-electrode cell with platinum as both the reference and counter electrodes and platinum or glassy carbon as the working electrode, with a scan rate of 2 mV/s.

2.5. Evaluation of capacitor performance

Performance of the electrolytes was tested in capacitors with carbon fiber cloth as the electrodes and the solutions of 1.0 and 2.0 m salt concentrations in γBL-AN solvents of varying compositions as the electrolyte. The carbon fiber cloth was provided to us gratis by Maxwell Technologies, from which pairs of electrodes of diameters of 1/2 and 7/16 in. were punched out. These electrodes were then assembled with two layers of a Cellguard as the separator into a coin-cell capacitor on a coin-cell assembly machine (W6A-3 by QPI Multipress, Inc.). Such capacitors were then measured for their impedance and cycled for their capacitance on a Solartron 1288-1266 impedance analyzer.

3. Results and discussion

3.1. Solid–liquid–vapor phase diagram of γBL-AN

The solvents AN and γBL, with their different boiling and melting points as listed in Table 1, form binary mixtures with a liquid range that changes with the solvent composition, as listed in Table 2 and shown in Fig. 1 [16]. As the γBL-AN phase diagram of Fig. 1 shows, this binary system has a eutectic temperature of −72.5° and a bubble point line that continuously rises from the boiling point of AN to that of γBL [8,10,11]. Thus, the addition of γBL in AN expands the liquid range of AN by not only raising its boiling point but also lowering its melting point. As an example, a mixture near the eutectic composition would have a liquidus temperature of −72.5 °C and a bubble point of 108 °C, an extension of about 30° from the liquid range of AN on both ends.

Closely associated with the boiling points of γBL and AN and the bubble points of their binary mixtures is the viscosity, η [8]. As these two liquids are reasonably similar in property, as evidenced by the change in the liquidus and bubble points and in the dielectric constant of γBL-AN mixtures as shown in Fig. 1 and later in Fig. 3, the η of their mixture is expected to change with its composition smoothly and monotonically from the η of one component to that of the other. Furthermore, η is expected to increase in value with a decreasing θ and an increasing salt content [8].

3.2. Solid–liquid ternary phase diagram of γBL-AN-Et_3MeNBF_4 with limited content in Et_3MeNBF_4

When Et_3MeNBF_4 was dissolved into the γBL-AN binary solvent to form the electrolyte, a ternary solution sys-

Table 2
Measured values of bubble point θ_b, liquidus temperature θ_l, and solidus temperature θ_s for the binary solvent $\gamma BL_{1-w}AN_w$ at different weight fractions w

w	θ_b (°C)	θ_l (°C)	θ_s (°C)
0.0000	204.8	−43.1	
0.1503	133.4		−72.5
0.2998	112.0		
0.3350		−72.5	
0.4448	100.1	−64.0	−72.5
0.5858	93.5	−57.8	−72.5
0.7299	87.8	−51.6	−72.5
0.8859	83.7	−46.1	−72.5
1.0000	81.2	−43.4	

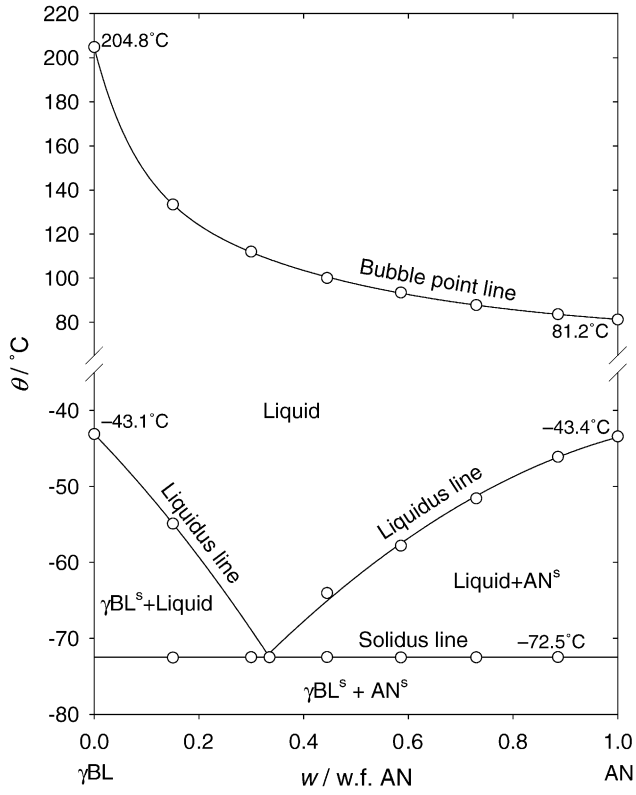

Fig. 1. Solid–liquid–gas phase diagram of the binary solvent system of γBL-AN, with the open dots representing the measured data and the curves those that have been fitted to the measured data. The liquid region, most relevant to the capacitor application, is bounded by the bubble point line on the upper temperature side and the liquidus line on the lower temperature side.

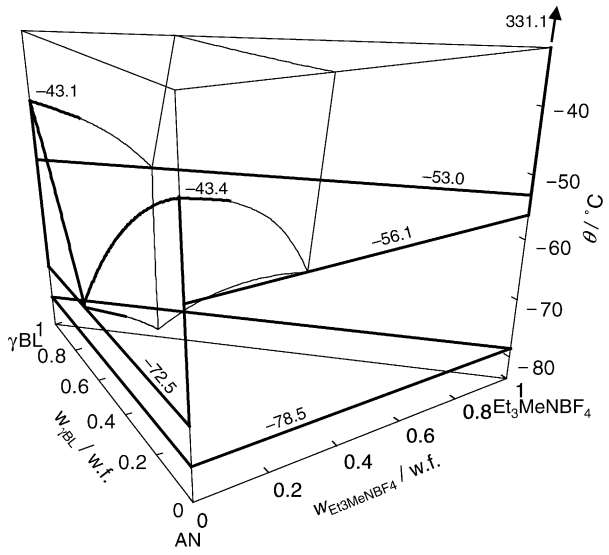

Fig. 2. Solid–liquid phase diagram of the ternary solution system γBL-AN-Et_3MeNBF_4 with a limited extent of Et_3MeNBF_4. The thick lines plot the experimental results and thin lines have been estimated or extrapolated. The number 331.1 on the arrow is the melting temperature of Et_3MeNBF_4 in °C.

tem resulted [15]. This system, like the γBL-AN solvent, was likely a simply eutectic ternary, even though its solid–liquid phase diagram was experimentally constructed only in the limited region poor in the salt, as shown in Fig. 2. However, owing to the invariant nature of the solidus transitions in the binaries γBL-Et_3MeNBF_4 and AN-Et_3MeNBF_4 and in the ternary γBL-AN-Et_3MeNBF_4, the eutectic temperatures, and therefore the solidus lines and the solidus plane, of these systems were experimentally obtained from the corresponding solvents and solution with the limited salt content, as indicated with the thick lines in Fig. 2. These lines show the eutectic temperatures of the two binaries with the salt (−56.1 and −53.0 °C) are only about 10° lower than the melting points of the two solvent components, while that of γBL-AN to be about 30° lower. This points clearly to the effectiveness of adding a solvent component to an electrolyte in lowering its liquidus temperature as compared to that of adding a salt, especially when the added solvent has a comparable melting point to that of the host solvent and the salt has a high melting point. This observation has its thermodynamic cause and therefore holds general applicability for electrolytes where the salts have much higher melting points than the solvents [13,15]. The ineffectiveness of adding a salt to a binary is more apparent in Fig. 2, as the eutectic temperature of the ternary is only 6° lower than that of the binary solvent.

3.3. Dielectric constant of γBL-AN binary solvent

Fig. 3 plots the results of ε measurement for the γBL-AN binary solvent at different temperatures, which shows ε of the solvent to decrease with w smoothly and monotonically from that of γBL to that of AN, and to increase with lowering θ, as has been observed in many other binary liquids [8]. In the figure, the open dots represent the measured data, and the curves plot their polynomial fitting function

$$\varepsilon = 45.188 - 0.14838\theta + 0.00028748\theta^2 - 3.5684w - 0.056855\theta w + 0.00020902\theta^2 w - 3.2189w^2 + 0.028451\theta w^2 + 1.3693w^3 \quad (1)$$

at the selected temperatures. This equation is also plotted as an ε-surface in the coordinates of w and θ, as inserted in the figure, to reveal the overall change of ε with these variables. As can be seen, this surface is a smooth and uncomplicated one slanting down from the axis of low θ and pure γBL, the component with the higher ε, to the axis of high θ and pure AN. A comparison of Fig. 3 and Fig. 1 clearly shows that the change of ε with w of a binary solvent is in the same direction as the change of its θ_b (and often its η). These have all been observed for many other solvent mixtures [8].

3.4. Conductivity of γBL-AN solution of Et_3MeNBF_4

Having learned the shape of the $\varepsilon(w, \theta)$ surface of the γBL-AN solvent (Fig. 3), and having known, based on the η-values

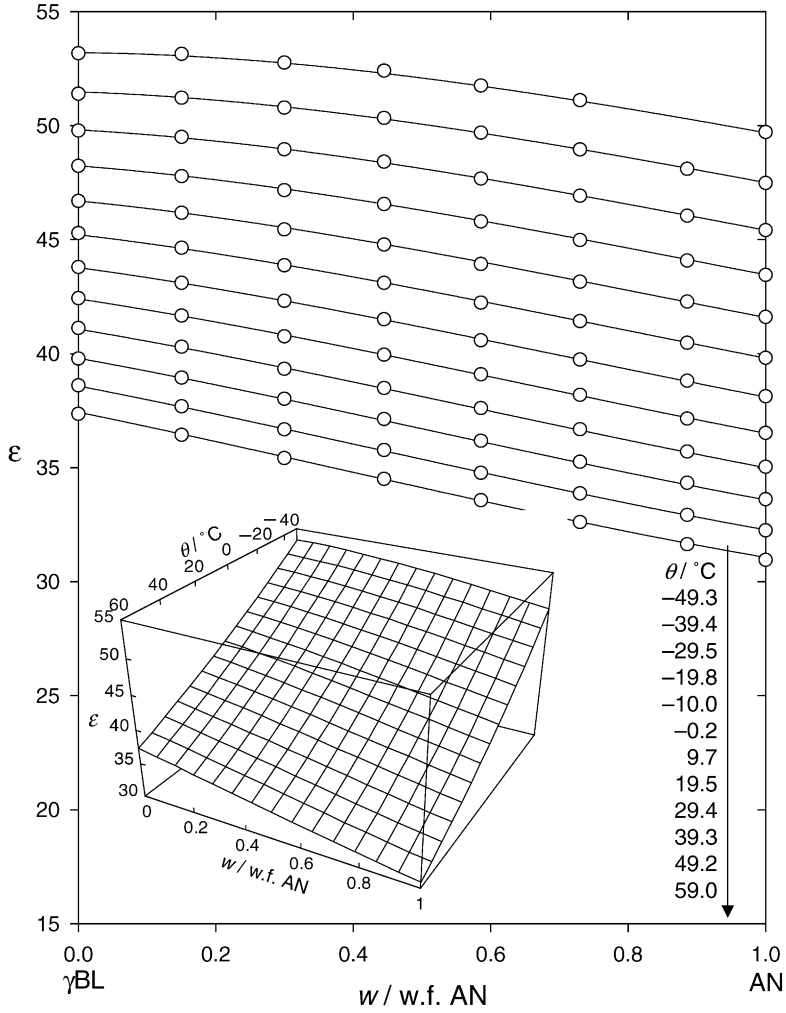

Fig. 3. Change of dielectric constant ε of γBL-AN binary solvent with its weight fraction w of AN and with temperature θ. The open dots represent the measured data, and the curves and the 3D surface plot the polynomial function of Eq. (1) that has been fitted to the measured data.

of γBL and AN and the way the η of their mixture would normally behave, that the η of the binary would increase with the γBL-content in the solvent, the salt content in the electrolyte, and a lowering θ, we are now in a position to anticipate how the $\kappa(m, w)$ surface of $(Et_3MeNBF_4)_m$-$\gamma BL_{1-w}AN_w$ solution would look like and how it would change with θ. As with every other liquid electrolyte, with an increasing m, κ should initially increase with the increasing number of the unassociated ions in the electrolyte, then level off, and finally fall, due to increases in η and in the number of associated ions in the electrolyte, generating a maximum κ (κ_{max}) at a particular m (m_{max}) in the process. With an increasing w, on the other hand, κ should increase initially because of a lowering η with the addition of AN. The added AN, however, also lowers the ε of the solvent, which may enable ions to pair up to such an extent that the κ of the electrolyte starts to fall, as has been observed many times in the Li^+-containing electrolytes of carbonate binary solvents where one component has a much smaller ε value than the other [27–30]. In view of the ε of AN being not much smaller than that of γBL (Table 1), the addition of AN in γBL may not cause a sufficient decline in the ε of the mixture to offset the decreasing η of the electrolyte for its κ to form a peak in w, as indeed occurred in the electrolyte system of $LiClO_4$ in propylene carbonate-AN binary [31]. In addition, an Et_3MeN^+ ion is so much larger than a Li^+ ion, which should further weaken the effect of ion association. It is therefore highly likely that the κ of the present electrolyte will peak in m but not in w.

These anticipations are largely fulfilled by the results of κ-measurement for the solution of $(Et_3MeNBF_4)_m$-$\gamma BL_{1-w}AN_w$, as plotted in Figs. 4 and 5. Fig. 4 plots the measured $\kappa(m)$ data with the open dots and their fitting function $\kappa(m, w, \theta)$ at the selected values of θ and w with the curves, while Fig. 5 plots the same function as $\kappa(m, w)$ surfaces at the selected values of θ. This fitting function is a trivariate polynomial function with 34 terms containing the variable m, w and θ, which, due to its unwieldy length, will not be given here but will be made available upon request. Suffice it to say that the fitting function described the measured data very accurately in the full ranges of m, w and θ

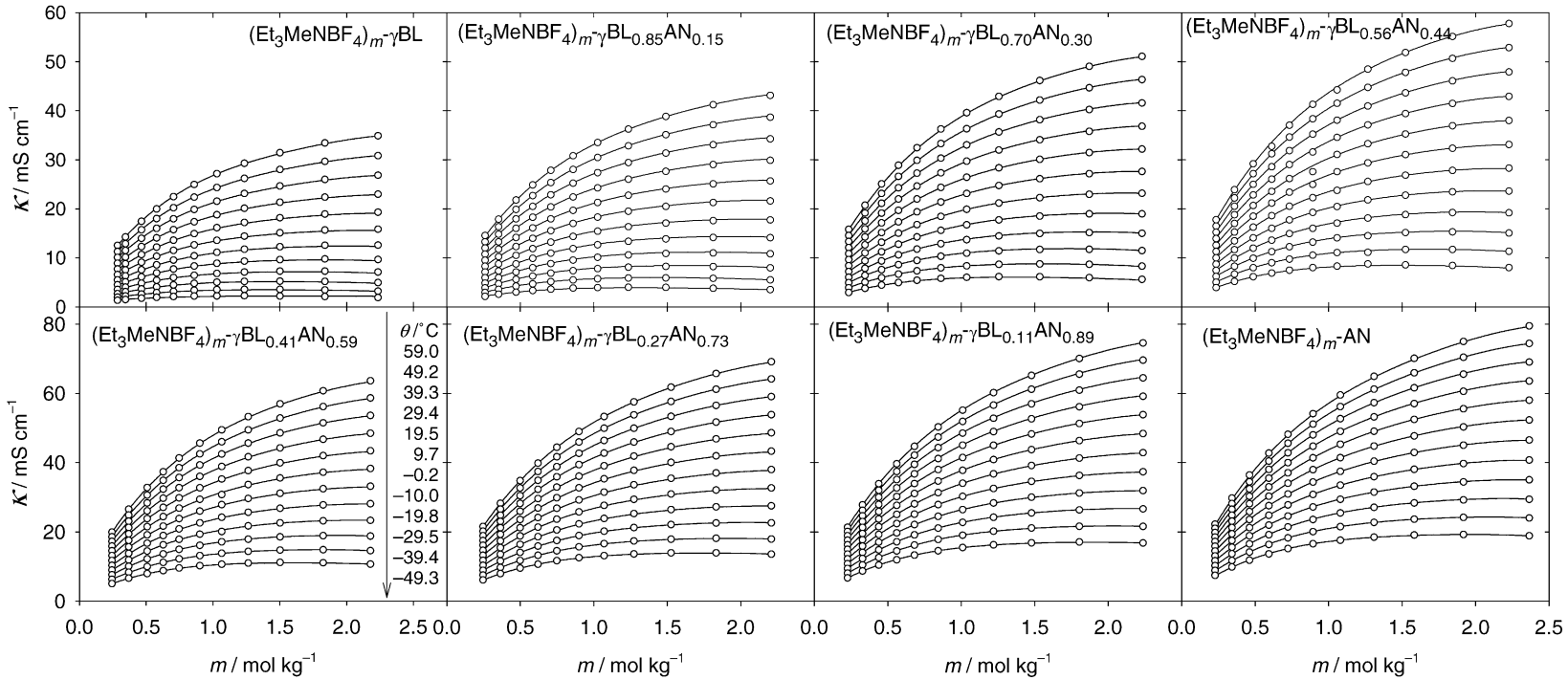

Fig. 4. Change of conductivity κ with salt molality m at different temperatures θ and solvent weight fraction w for $(Et_3MeNBF_4)_m$-$\gamma BL_{1-w}AN_w$ solution. The open dots represent the measured data and the curves plot their polynomial fitting function $\kappa(m, w, \theta)$.

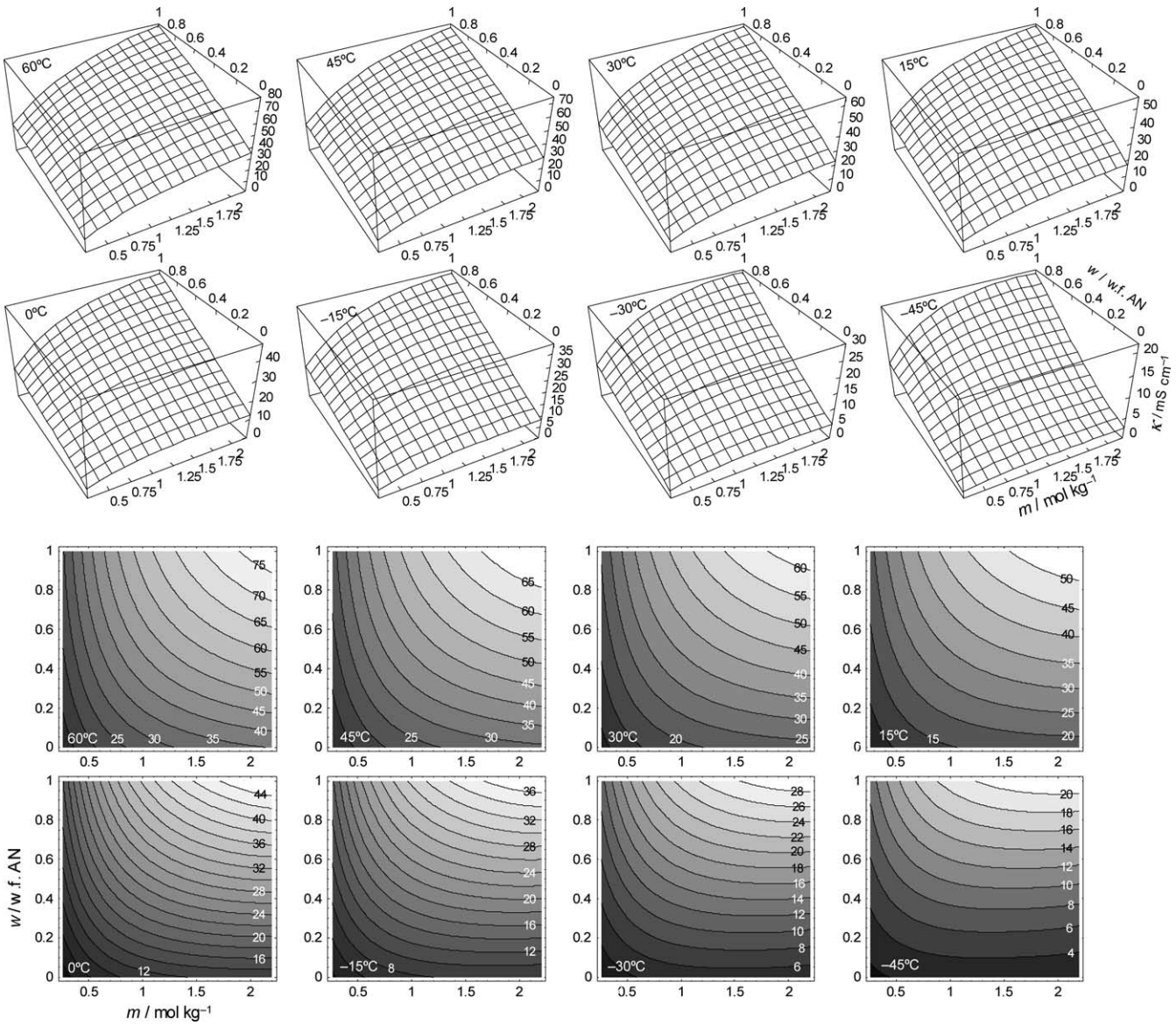

Fig. 5. Change of conductivity κ with simultaneous changes in salt molality m and solvent weight fraction w for $(Et_3MeNBF_4)_m$-$\gamma BL_{1-w}AN_w$ solution according to their polynomial fitting function $\kappa(m, w, \theta)$. Each function is doubly represented by a surface plot (upper plots) and a contour plot (lower plots) with the temperatures and the contour values indicated in the plots.

of the experiments. An important reason for this function to be able to faithfully describe even the measured $\kappa(m)$ data was that these data did not extend much beyond the m_{max}, as can be seen in Fig. 4. A set of measured $\kappa(m)$ data extending considerably beyond the m_{max} has been known to be very difficult to fit with a polynomial function; such cases would have called for the use of the Casteel-Amis equation and its extended versions [27–30,32].

As shown in Figs. 4 and 5, the κ of the $(Et_3MeNBF_4)_m$-$\gamma BL_{1-w}AN_w$ solution indeed peaks in m at low temperatures, although the values of m_{max} are rather high and the peaks are rather broad compared to Li^+-containing electrolytes. However, the κ rises steadily with w from pure γBL all the way to pure AN, thus failing to form a peak in w. This is primarily the result of the η of the $\gamma BL_{1-w}AN_w$ solvent decreasing significantly with w, in combination with its ε decreasing only slight with w and the weak tendency for association between the Et_3MeN^+ and BF_4^- ions. The change of κ with θ is just as usual: the $\kappa(m, w)$ surface decreases in height with a lowering θ, as shown in Fig. 5. Thus, these surfaces are neither dome- nor arch-shaped, as those of other solution systems are, but rather assume a combination form of a low-θ arch transitioning to a high-θ slope, as seen in Fig. 5.

Maximum conductivity with respect to m, κ_{max}, and the particular m at which this maximum occurs, m_{max}, were calculated from the polynomial function $\kappa(m, w, \theta)$ that has been fitted to the experimental data and plotted in Fig. 6 to show their change with w and with θ. As shown, both the κ_{max} and m_{max} increases with w demonstrating the effect of a decreasing η in the solvent in delaying the onset of the decline

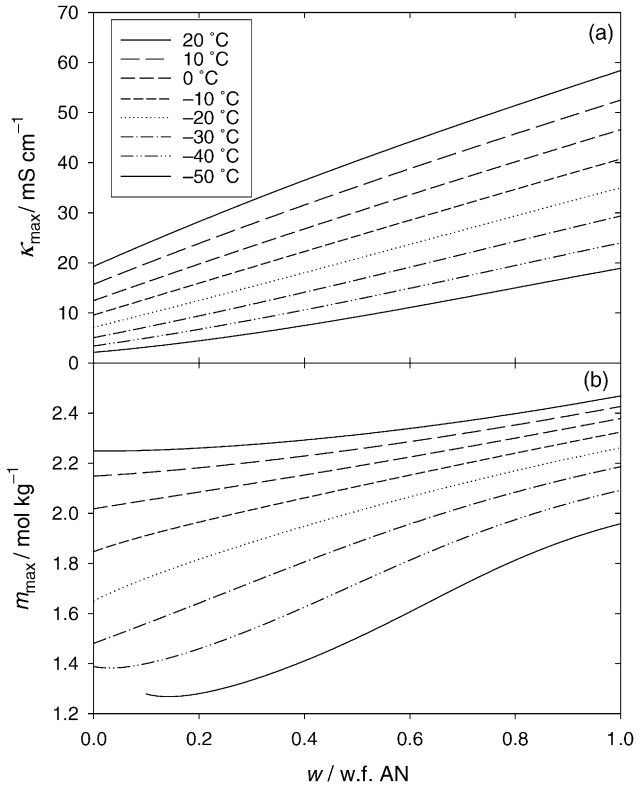

Fig. 6. Change of the salt molality m_{max} (a) with the solvent weight fraction of w, according to the polynomial fitting function $\kappa(m, w, \theta)$, (b) at which the conductivity of $(Et_3MeNBF_4)_m$-γ$BL_{1-w}AN_w$ solution reaches its maximum κ_{max}.

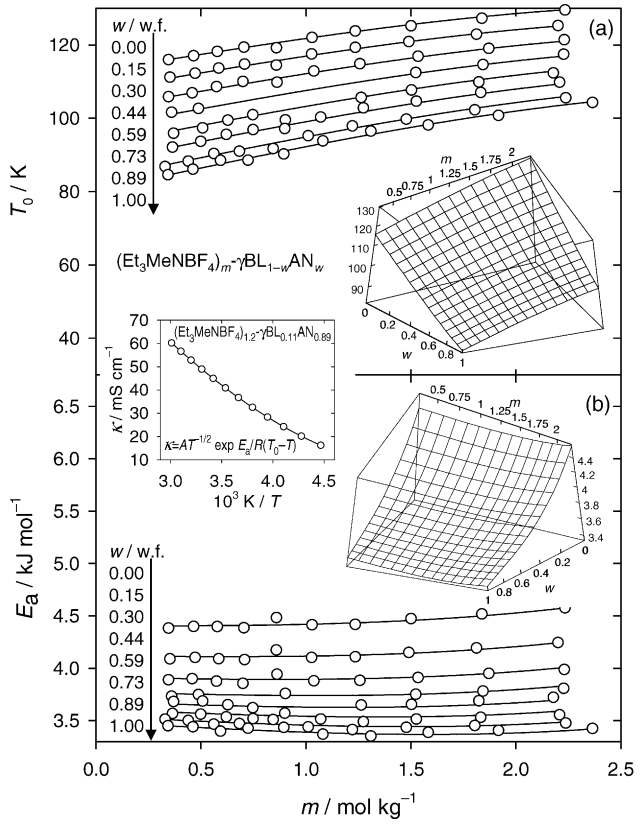

Fig. 7. Results of fitting the measured $\kappa(T)$ data with the VFT equation for $(Et_3MeNBF_4)_m$-γ$BL_{1-w}AN_w$ solution at different salt molalities m and solvent weight fractions w. The plots (a) and (b) describe, respectively, the vanishing mobility temperature T_0 and the apparent activation energy E_a, with the open dots representing the fitting results and the curves and the surfaces representing polynomial functions that hiave been fitted to the open dots.

in κ with m due to an increase in η of the electrolyte and in enhancing the conduction of ions. In addition, vanishing mobility temperature, T_0, and apparent activation energy, E_a, have been calculated from the measure $\kappa(T)$ data, and plotted in Fig. 7 as both 2D curves and 3D surfaces, to show the change of these parameters with w. Of particular relevance is the surface of T_0 in Fig. 7a, which can be viewed as a reflection of η of the corresponding electrolytes, as a higher T_0 is usually associated with a higher η for similar liquids. As such, Fig. 7a can be seen as a confirmation for the earlier assertion regarding the change of η of the electrolyte: T_0 surface simply slants up from the corner of low m and high w to that of high m and low w.

3.5. Variation of electrochemical stability with solvent composition

Results of measurement on the electrochemical stability window of the solvents of different compositions are plotted in Fig. 8 in the form of voltammetric curves. These curves show that the oxidative stability of the solvent generally improves with increasing content of γBL, or a decreasing w, with progressively higher threshold voltage value for the oxidation of the solvent, as seen in Fig. 8a with a platinum working electrode. Fig. 8b shows, with a glassy carbon wording electrode, a similarly widening electrochemical stability window, and a progressively suppressed current peak likely associated with a decomposition of a solvent component on the carbon surface.

3.6. Properties and performance of capacitors

In the operation of a double-layer capacitor, the charge and discharge processes involve only the migration of ions in the electrolyte, through a separator if one is present, but do not involve the charge transfer at the electrolyte–electrode interface and the insertion and extraction of ions into and from the electrode lattice, as the same processes in a battery do. As such, the κ of the electrolyte is much more directly related to the resistance of a capacitor than of a battery, and its change is thus expected to have strong impact on the performance of the capacitor. To observe this impact, electrolytes of $(Et_3MeNBF_4)_{2.0}$-γ$BL_{1-w}AN_w$ of different w's were used as the electrolytes for a series of coin-cell capacitors, with a carbon cloth as the electrodes and a double-layered cellguard as the separator. These capacitors were measured for their equivalent series resistance, R_{es}, with an impedance analyzer, and the results are plotted in Fig. 9 as functions of w

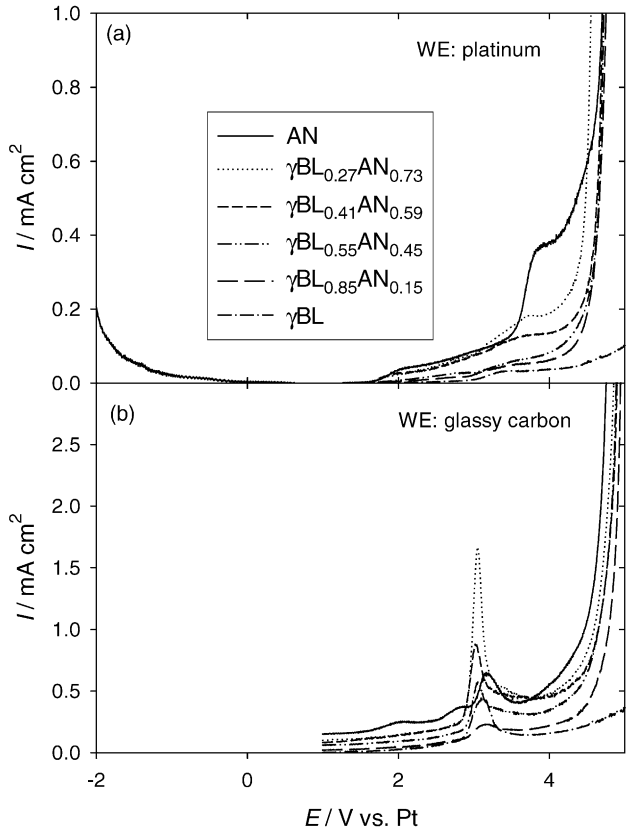

Fig. 8. Electrochemical stabilities against oxidation of γBL-AN binary mixtures, on the surfaces of platinum (a) and glassy carbon (b), both with a scan rate of 2 mV/s.

at different θ's. As the figure shows, R_{es} decreases with w and with increasing θ, the speed with which it does so with w rising up with decreasing θ. These trends have their exact counterparts in the change of κ of the electrolytes with the same variables, as seen in Figs. 4 and 5.

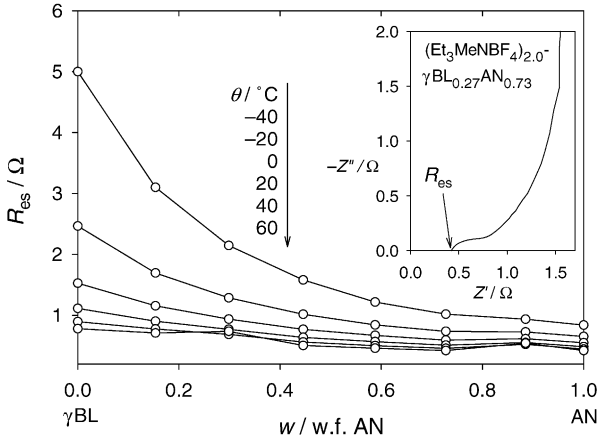

Fig. 9. Change of equivalent series resistance R_{es} with solvent composition w and with temperature θ of capacitors containing $(Et_3MeNBF_4)_{2.0}$-$\gamma BL_{1-w}AN_w$ as the electrolyte. The insert in the upper plot shows an impedance curve of a capacitor with $(Et_3MeNBF_4)_{2.0}$-$\gamma BL_{0.27}AN_{0.73}$ electrolyte and the manner in which the R_{es} of the capacitor was determined.

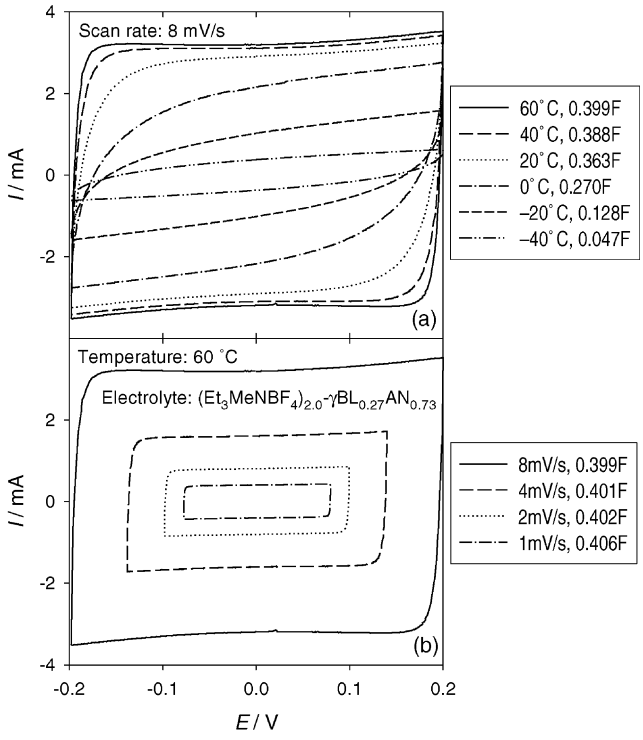

Fig. 10. Cyclic voltammograms of capacitors containing $(Et_3MeNBF_4)_{2.0}$-$\gamma BL_{0.27}AN_{0.73}$ as the electrolyte, to demonstrate the determination of their capacitance and its variation with temperature and with scan rate.

Fig. 10 gives some cyclic voltammograms as examples for the performance of the capacitors. Fig. 10a plots the effect of θ on the behavior and the capacitance of a capacitor, at a scan rate of 8 mV/s. It can be seen that at higher θ's, the capacitor behaves like a perfect capacitor, with symmetrical charge and discharge currents and constant values of capacitance. But at lower θ's, with a higher R_{es}, the voltammograms depart more and more from a square, and the capacitance falls noticeably. These properties are similarly affected by the scan rate at a fixed θ, as shown in Fig. 10b. Here, the effects of a higher rate are the same as those of a lower temperature.

Correlation of the electrochemical stability of the electrolytes, as shown in Fig. 8, with the operating voltage of the capacitors containing the electrolytes, is shown in Fig. 11 with the voltage profiles of three capacitors each charged to successively higher voltages with a constant current [16]. As shown in Fig. 11a, the capacitor with AN as the solvent was successfully operated up to 2.5 V, but failed at 3.0 V due to the decomposition of the solvent. When the solvent was changed to half AN and half γBL by weight, the decomposition voltage of the solvent in the capacitor was raised to above 3.0 V (Fig. 11b). When the solvent was pure γBL, this decomposition voltage was further increased to above 3.5 V (Fig. 11c). This increase in the operating voltage of the capacitors with the γBL content in the solvents of the capacitors clearly corresponds to the general increase in the oxidative potential with the γBL content in the γBL-AN binary solvents shown in Fig. 8.

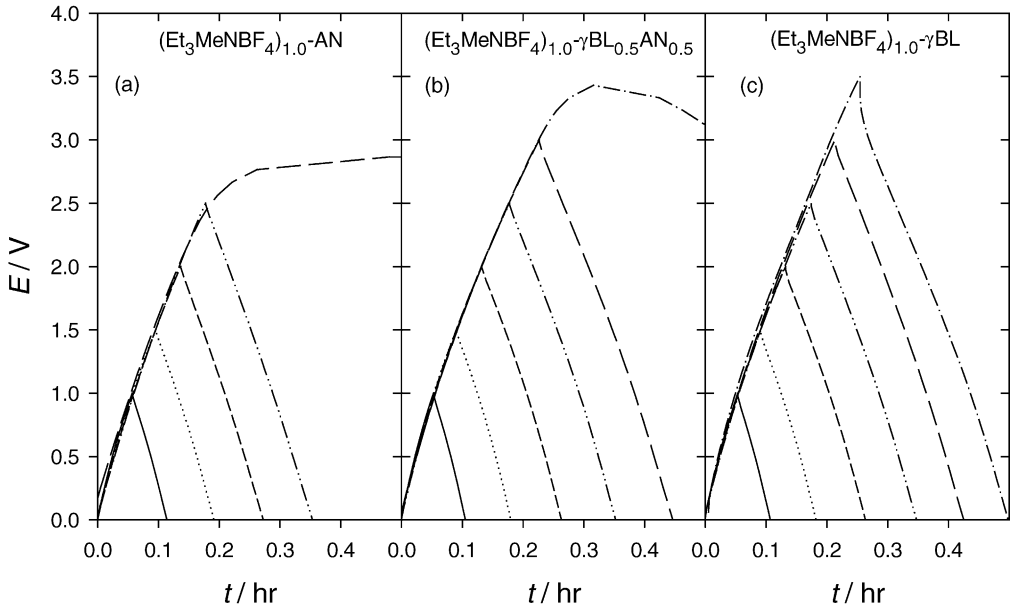

Fig. 11. Voltage profiles E in time t of the capacitors with the electrolytes of 1.0 m Et_3MeNBF_4 in AN (a), γBL (c), and a mixture of the two (b), charged to successively higher voltages with a constant current of 2.0 mA cm^{-1}, for the observation of the change of operating voltage with the solvent composition.

4. Conclusions

The properties of the solution of a quaternary ammonium salt in a binary non-aqueous solvent can be effectively optimized for use as an electrolyte for double-layer capacitors by choosing an appropriate salt and solvent and by properly adjusting the composition of the solution. For the particular solution of Et_3MeNBF_4 in γBL-AN binary solvent studied here, addition of γBL in AN expanded the liquid range of AN significantly on both sides of the temperature range. Furthermore, the lowering of the liquidus temperature by the addition of the solvent was much more effective than by the addition of the salt, especially when the added solvent had a comparable melting point to, and the salt had a much higher melting point than, the host solvent. For dielectric constant, the addition of γBL in AN resulted in a continuous rise in value, while an increase in temperature caused a universal decline. Conductivity of the γBL-AN solution of Et_3MeNBF_4 peaked in salt content but rose continuously with the AN content in the solvent. Oxidative stabilities of the solvents at different solvent compositions showed a general improvement with the γBL content. In correlation to these changes in the property of the solution, the double-layer capacitors utilizing this solution as their electrolytes demonstrated an equivalent series resistance and an operating voltage that rose in value with the γBL content in the solvent.

References

[1] B.E. Conway, Electrochemical Supercapacitors: Scientific Fundamentals and Technological Applications, Kluwer Academic/Plenum Publishers, New York, 1999.
[2] A. Burke, J. Power Sour. 91 (2000) 37–50.
[3] M. Zolot, B. Kramer, Proceedings of the 12th International Seminar on Double-Layer Capacitors and Similar Energy Storage Devices, Deerfield Beach, December 2002.
[4] A. Chu, P. Braatz, J. Power Sour. 112 (2002) 236–246.
[5] J.P. Zheng, T.R. Jow, M.S. Ding, IEEE Trans. Aero. Electr. Sys. 37 (2001) 288–292.
[6] M. Arulepp, L. Permann, J. Leis, A. Perkson, K. Rumma, A. Janes, E. Lust, J. Power Sour. 133 (2004) 320–328.
[7] M. Morita, Y. Matsuda, J. Power Sour. 60 (1996) 179–183.
[8] M.S. Ding, J. Electrochem. Soc. 150 (2003) 455–462.
[9] S.P. Ding, K. Xu, S.S. Zhang, T.R. Jow, K. Amine, G.L. Henriksen, J. Electrochem. Soc. 146 (1999) 3974–3980.
[10] M.S. Ding, K. Xu, T.R. Jow, J. Electrochem. Soc. 147 (2000) 1688–1694.
[11] M.S. Ding, K. Xu, S.S. Zhang, T.R. Jow, J. Electrochem. Soc. 148 (2001) 299–304.
[12] M.S. Ding, K. Xu, T.R. Jow, J. Therm. Anal. Calorim. 62 (2000) A177–A186.
[13] M.S. Ding, J. Electrochem. Soc. (2002) 149.
[14] Z.K. Liu, J. Electrochem. Soc. 150 (2003) 359–365.
[15] M.S. Ding, J. Electrochem. Soc. 151 (2004) 731–738.
[16] T.R. Jow, M.S. Ding, K. Xu, Extended Abstracts of 2003 International Conference on Advanced Capacitors, Kyoto, May 2003.
[17] D.R. Lide (Ed.), CRC Handbook of Chemistry and Physics, 84th ed., CRC Press, Boca Raton, Florida, 2004.
[18] J. Barthel, R. Neueder, R. Meier (Eds.), Chemistry Data Series, vol. XII, DECHEMA, Frankfurt, 1997, p. 442.
[19] V. Gutmann, Electrochim. Acta 21 (1976) 661–670.
[20] M. Ue, K. Ida, S. Mori, J. Electrochem. Soc. 141 (1994) 2989–2996.
[21] B.E. Conway, J. Electrochem. Soc. 141 (1994) 2989–2996 (Chapter 13).
[22] M. Ue, M. Takeda, M. Takehara, S. Mori, J. Electrochem. Soc. 144 (1997) 2684–2688.
[23] K. Xu, M.S. Ding, T.R. Jow, J. Electrochem. Soc. 148 (2001) A267–A274.
[24] M. Ue, M. Takehara, M. Takeda, Denki Kagaku 65 (1997) 969– 971.

[25] S.P. Ding, K. Xu, T.R. Jow, Selected Battery Topics, , in: G. Halpert, M.L. Gopikanth, K.M. Abraham, W.R. Cieslak, W.A. Adams (Eds.), Electrochem. Soc. Proc. Series, vol. PV98-15, Pennington, New Jersey, 1999.
[26] I. Mills, T. Cvitas, K. Homann, N. Kallay, K. Kuchitsu, Quantities, Units and Symbols in Physical Chemistry, 2nd ed., IUPAC and Blackwell Scientific Publications, London, 1993.
[27] M.S. Ding, J. Chem. Eng. Data 48 (2003) 519–528.
[28] M.S. Ding, T.R. Jow, J. Electrochem. Soc. 150 (2003) 620–628.
[29] M.S. Ding, J. Electrochem. Soc. 151 (2004) 40–47.
[30] M.S. Ding, K. Xu, T.R. Jow, J. Electrochem. Soc., in press.
[31] J. Barthel, R. Neueder, M. Poxleitner, J. Seitz-Beywl, L. Werblan, J. Electroanal. Chem. 344 (1993) 249–267.
[32] J.F. Casteel, E.S. Amis, J. Chem. Eng. Data 17 (1972) 55–59.